

The Numerical Simulation of a Staged Transverse Injection behind a Rearward Facing Step into a Mach 2 Stream in a Confined Environment

¹John Vivian Prashant and ²Kuldeep Sharma

^{1,2} Bachelor of Technology Students, Department of Aerospace Engineering, Indian Institute of Space Science & Technology, Valiyamala, Trivandrum, Kerala, India, 695547.

Abstract: The primary aim of this work was to carry out the numerical simulation of a staged transverse injection behind a rearward facing step into a Mach 2 stream in a confined environment. This problem has been investigated experimentally by McDaniel et al. And the same conditions have been recreated for the numerical simulation. An extensive and in-depth comparison of the numerical predictions with the experimental results has been presented through plots of various flow parameters at different locations in the test section. The numerical results show an excellent agreement with the experimental results. Deviations from the experimental results are also observed in some scenarios due to the inability of the numerical schemes to capture the effects of shocks and expansion fans. Efforts to study the nature and cause of these deviations have also been made. This particular cold flow mixing problem has been completely analysed and has been solved numerically using k - ω (SST) and realizable k - ϵ viscous models. The flow parameters have been analysed and plotted for both with and without injection cases. The mixing has been performed using both with and without species utility of the software. The main focus of this work is to try to understand the mixing of the fuel and air in the combustion chamber. Good mixing is the most important prerequisite for good combustion. The central focus has been laid on trying to understand the staged transverse injection technique of mixing.

Keywords--- Supersonic mixing, Scramjet, Transverse Injection, Numerical Simulation

I. INTRODUCTION

Basically a scramjet is a variant of a ramjet engine in which the combustion process takes place in supersonic airflow. This allows the scramjet to efficiently operate at extremely high speeds.

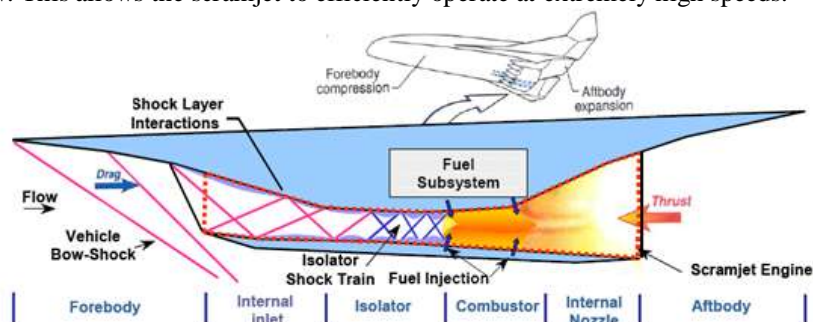


Fig. 1: General Components of a Scramjet engine
(Picture taken from NASA website on 20 sep 2010)

Hypersonic flight within the atmosphere generates enormous drag and high temperature. Within the engine the temperature can be nearly six-times greater than that of the surrounding air. Maintaining combustion in the supersonic flow presents many challenges such as injection, mixing, ignition, and burning within very short duration of time. Mixing, Ignition and flame holding in a scramjet combustor are the major challenges in a scramjet operation. At high speeds when air enters in the combustion chamber its temperature increases due to shock interactions. And if the flow becomes subsonic the temperature increases to an extent that it causes dissociation of air molecules which is an endothermic reaction. This leads to inefficient heat addition. Due to this enough transitional kinetic energy isn't imparted to the molecules and the thrust decreases. This is the reason to adopt supersonic free stream in the combustion chamber of scramjets. Recirculation regions are used for flame holding because of subsonic Mach numbers in these regions. Supersonic combustion involves turbulent mixing, shock interaction and heat release in supersonic flow. The flow field within the combustor of

scramjet engine is very complex and causes a lot of difficulties in the design and development of a supersonic combustor with an optimized geometry. Efficient combustors should promote sufficient mixing of the fuel and air so that the desired chemical reactions can take place [1],[2].The 2 basic approaches for verification of scramjet design are Ground test facilities and Numerical simulations. Ground tests alone cannot give data with sufficient accuracy for design of hypersonic systems. Due to the complex nature of the problems component level testing will not be able to simulate accurately the complex flow field. Also, the quality of air is difficult to simulate in the test facilities. Therefore there is a need to estimate the flight performance based on the results of ground tests. This can be accomplished only through the use of mathematical modelling of the flow, which is to be solved to first reproduce the result of the ground test and then used for predicting the flight conditions. Numerical computation involves evolving algorithms to solve the Navier Stokes equations or their variants such that sharp gradient regions near the shocks are captured with numerical diffusion or overshoot. The prediction of wall heat transfer rate. The advantage of mathematical model is that once it is validated it can be used to conduct several numerical experiments with various modifications of flow parameters. Also, they are much less expensive compared to experiments. This is the current day approach to find solutions to the problems of high-speed flight.

II. Transverse Injection:

The fuel is injected perpendicular to the flow direction. The penetration of the fuel into the flow decides the extent of mixing. Mixing is more when the penetration is higher. But due to the obstruction of the flow by the injectant, bow shocks are produced which hinder the mixing.

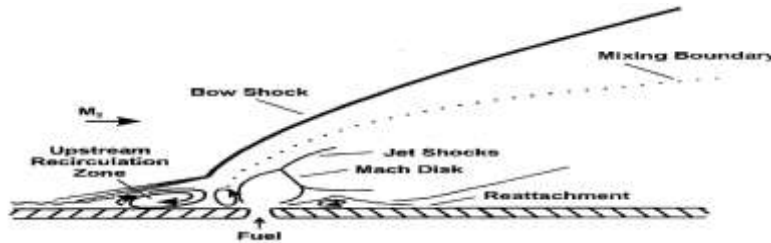


Fig. 2: Transverse Injection

III. DESCRIPTION OF THE EXPERIMENT

Flow field description of the experiment conducted by James C. McDaniel, Douglas G. Fletcher, Roy J. Hartfield and Steven D. Hollo is as follows: The air supply for the wind tunnel used for the non-reacting measurements in this experiment consisted of a centrifugal air compressor (0.75kg/sec maximum output) and 56.6 cubic meters of high pressure (2.07 MPa) storage volume. The air was filtered and dried to a nominal dew point of -56 C. Nominal tunnel stagnation conditions were 300 K and 274 kPa [2].

TABLE 1
FLOW PARAMETERS

PARAMETER	TUNNEL	INJECTOR
P_o	274 KPa	263 KPa
T_o	300 K	300 K
M	2 (test section inlet)	1 (exit)
P_{inf}	35 KPa (free stream)	139 (exit)
T_{inf}	167 K (free stream)	250 (exit)
U_{inf}	518 m/s (free stream)	317 m/s (exit)
Mass Flow Rate	0.2 kg/s	1.64 g/s

The same conditions have been recreated for numerical analysis on FLUENT.

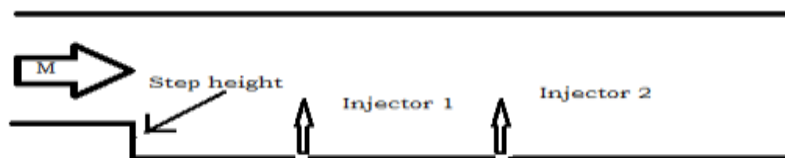


Fig. 3: Schematic diagram of the experimental setup

IV. TURBULENCE MODELLING

Turbulent Flows are characterized by a fluctuating velocity field (in both position and time).The velocity field is random.

SST K-Omega Model

The SST k- ω turbulence model is a two-equation eddy-viscosity model. The SST k- ω model can be used as a Low-Re turbulence model without any extra damping functions.

K-Epsilon Model

It is a two equation model containing two extra transport equations to represent the turbulent properties of the flow. It is useful for free-shear layer flows with relatively small pressure gradients and for internal flows.

V. COMPUTATIONAL DETAILS

The grid independence test has been performed confirming convergence of the numerical result using three different grids of 212250 cells, 383832 cells and 533700 cells.The grids are fine near the wall and backward facing step region and relatively coarse in the outward region.

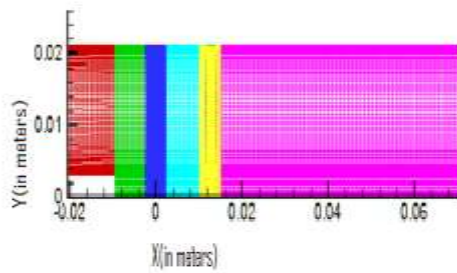


Fig. 4: Mesh structure for 383832 cells

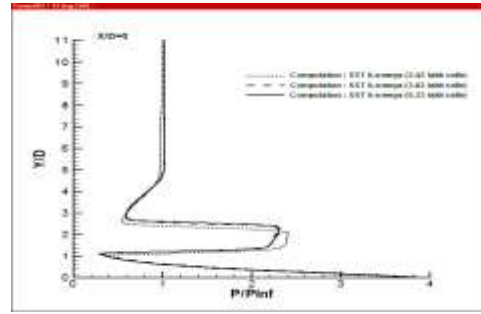


Fig. 5: Grid Independence

Test

TABLE 2
Details & Default Model Constants of Fluent Analysis Conditions

SOLVER	Density based, Explicit, 3D, Steady, Velocity formulation (absolute), Gradient option (Green Gauss cell based), Porous formulation (Superficial velocity)	
VISCOUS MODELS	SST K-OMEGA	Alpha*_inf=1,Alpha_inf=0.52 ,Beta*_inf=0.09 ,R_beta=8,Zeta*=1.5, Mt_o=0.25, a1=0.31,Beta_i(Inner)=0.075,Beta_i(Outer)=0.082,TKE (Inner)Prandtl#=1.176,TKE (Outer)Prandtl=1, SDR (Inner)Prandtl#=2,
	REALIZABLE K-EPSILON (2 EQN)	C2-Epsilon=1.9, TKE Prandtl Number=1,TDR Prandtl Number=1.2, Energy Prandtl Number=0.85,Wall Prandtl Number=0.85,Turb. Schmidt Number=0.7, Near wall treatment= Standard wall functions
	SPALART-ALLMARAS (1 EQN)	Cb1=0.1355, Cb2=0.622,Cv1=7.1,Cw2=0.3,Cw3=2,Prandtl Number=0.667,Energy Prandtl Number=0.85,Wall Prandtl Number=0.85,Turb. Schmidt Number=0.7
OPERATING CONDITIONS	Operating pressure (Pascal) =0	
BOUNDARY CONDITIONS	INJECTION HOLE	Gauge total pressure=263000 Pa Supersonic/initial gauge pressure=139000 Pa

	INFLOW	Gauge total pressure=274000 Pa Supersonic/initial gauge pressure=35000 Pa
	OUTLET	Gauge pressure=35000 Pa

V. RESULTS

Flow field was simulated using FLUENT for both with and without injection cases and different parameters like P/P_{inf} , T/T_{inf} , U/U_{inf} , and Mole fraction of injectant were plotted at different X/D (axial) locations. Results obtained from computational analysis were compared with experimental results taken from the paper by McDaniel et al. These plots and contours are given in appendix. It has been observed that computational results are well matching with experimental results and error is within 10%. The deviation from experimental results is due to the limitations of the viscous model to exactly model the real problem and errors involved in computation. Here we have used 2 equation models (SST k-omega & k-epsilon) for turbulence modelling. A major assumption of almost all two-equation models is that the turbulent fluctuations, u' , v' , and w' , are locally isotropic or equal. This is true for the smaller eddies at high Reynolds numbers. The large eddies are in a state of steady anisotropy. But here in this flow situation Mach number is pretty high so eddies are generated. So due to eddies two equation models are not able to capture exact phenomenon and that's why experimental and computational results are not same. First of all a grid independence study was carried out using SST k-omega viscous model and it was found that results become independent of grid size after around 3.83 lakh cells. So results were plotted for 3.83 lakh cells. From Figure 6, 7, 8, 9, 10, 11 we can clearly see that as X/D increases penetration of injectant (air) into the free stream increases because air is injected into the free stream near $X/D=0$, so as X/D increases air is mixed with free stream and more penetration takes place. This happens due to vortex creation which lifts the plume from surface to core and hence plume spreads. From these figures we can see that computational results (left part of figure) are matching with experimental results (right part of the figure). In figure 12 & 13 expansion fan, reattachment shock and barrel shock regions can be seen clearly. Figure 14 shows the velocity profile in test section and recirculation region near the step can be seen clearly. Figure 15 shows the mole fraction spread of the injectant (air). It's evident from the contour plot that eventually as X/D increases mixing of free stream and injectant (air) takes place. In a similar way Fig16, 17 & 18 represent shocks, velocity profile, recirculation region etc. in test section without injection. Different viscous models were used to solve the problem. Spalart-Allmaras & SST k-omega was used to solve without injection case and SST k-omega & Realizable k-epsilon were used for with injection case. Comparison of SST k-omega and Spalart-Allmaras is shown in Fig19 and it can be clearly seen that both models give very good prediction of actual problem. So we can use any one of the models for this problem. Fig26 shows a comparison between SST k-omega and Realizable k-epsilon and it can be clearly seen that k-omega gives better results near the wall. This is because SST (shear stress transport) k-omega model is capable of capturing the physical phenomenon near the wall which is because of shear stress. K-omega model resolves viscous sub layer without any significant error. K-epsilon model doesn't give very good results near the wall even after using the wall function (standard wall function). So to capture the phenomenon in viscous sub layer we have to use a more powerful wall function along with the k-epsilon model.

Figure 20 P/P_{inf} & T/T_{inf} at $X/D=-2.05$ shows the effect of recirculation region. The temperature decreases and the pressure almost remains constant near the wall. Figure 21 shows pressure and temperature variation along transverse direction at $X/D=0$ for without injection case. As Y/D increase from 0 to 2, pressure decreases because of expansion fan encountered. As y/D increases from 2 to 5 pressure starts to increase because of reattachment shocks and after that pressure becomes equal to free stream pressure. Same trend is observed for temperature also. Similar phenomenon is observed in Figure 22. Figure 23-25 show the variation of mole fraction of injectant at different X/D locations. Figure 27-30 show the P/P_{inf} , T/T_{inf} at various X/D locations. Effects of expansion fans & reattachment shocks can be clearly seen on these parameters from these plots.

VI. CONCLUSION

Commercially available software's Gambit and Fluent were used to carry out meshing and simulation of the flow over a rearward facing step. Also simulations were carried out along with staged transverse injections. Simulations results for without injection and with injection cases were compared with results taken from experiments conducted by McDaniel et al. It was found that computation results were closer to the LIIF

results than PLIIF. Some deviations were noticed in computation and experimental results due to the inability of the numerical scheme to simulate the real flow. This happens because of the reason that numerical scheme tries to build a mathematical model of the real problem, which is never exactly same as of the real problem. The FLUENT software was efficient in capturing the overall essence of the problem taken up. The staged transverse injection gives good mixing but still more modifications could be made to enhance mixing further. The optimal gridding and selection of the relevant mathematical models is very necessary for achieving clear and accurate results. It is also very important to select the correct mathematical models on the numerical solvers to ensure accurate results. Numerical methods provide more freedom and agility to carry out hypersonic tests at an affordable price. But proper evaluation of the software's capacity to predict correct results should be done.

References

- [1] D Chakraborty, A. P Roychowdhury, V. Ashok and P. Kumar .Numerical investigation of staged transverse sonic injection in Mach 2 stream in confined environment. *Aeronautical Journal*,2003,107(1078), 719-729.
- [2] McDaniel, J.C., Fletcher, D., Hartfield, R. and Hollo, S. Staged transverse injection into Mach 2 flow behind rearward facing step: a 3D compressible test case for hypersonic combustor code validation,1991,AIAA paper No 91-5071.

APPENDIX

1) Contour plots for cross-flow injectant mole fraction distribution

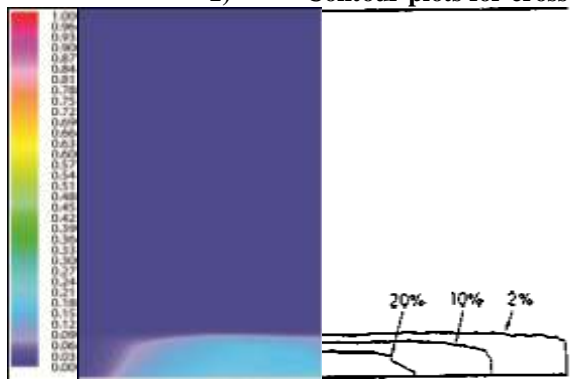


Fig6:-X/D=-3

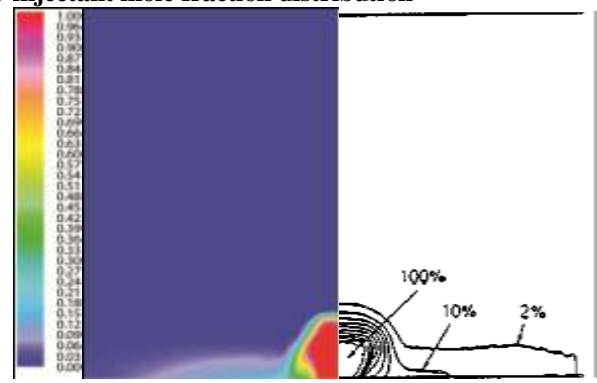


Fig7:-X/D=0

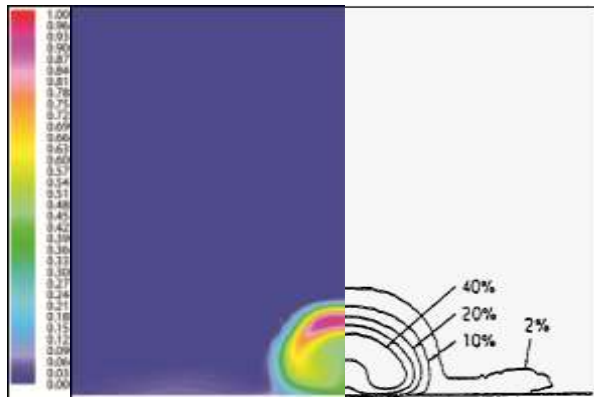


Fig8:-X/D=3

X/D=9

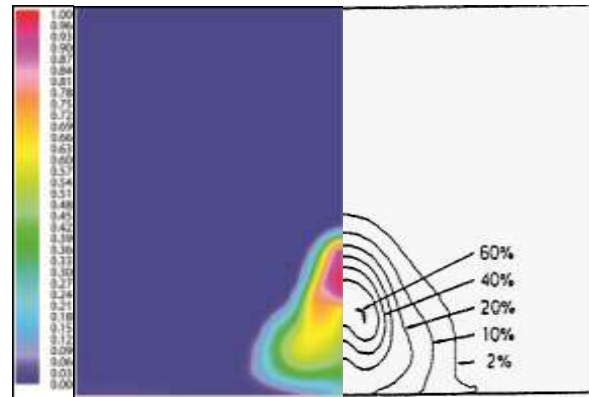


Fig9:-

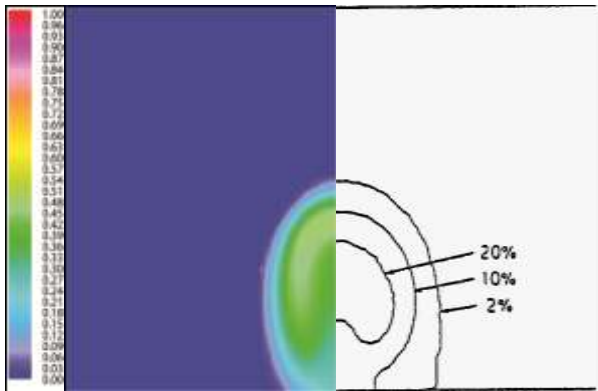


Fig10:-X/D=18

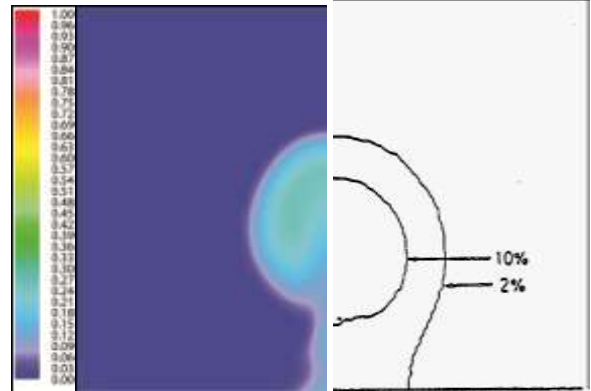


Fig11:-X/D=30

2) CONTOURS

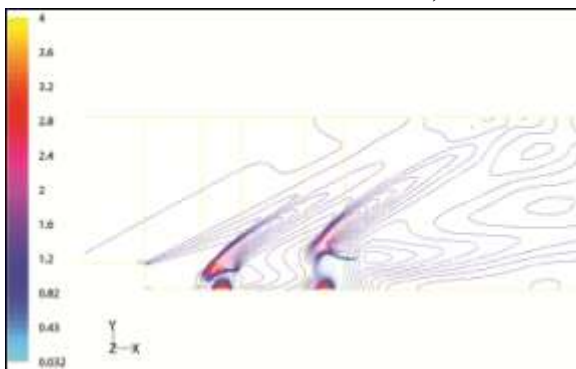


Fig12 :- P/P0 (with injection)

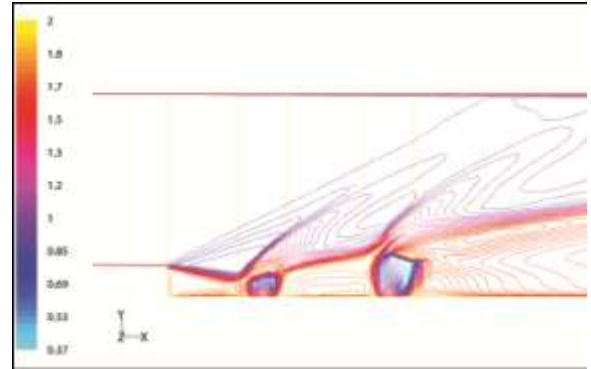


Fig13 :- T/T0 (with

injection)

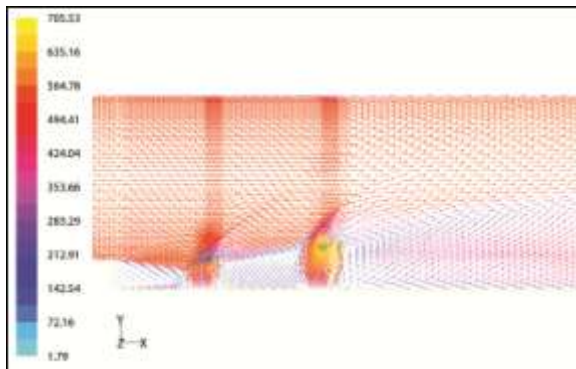


Fig14:- Velocity vector plot (with injection)

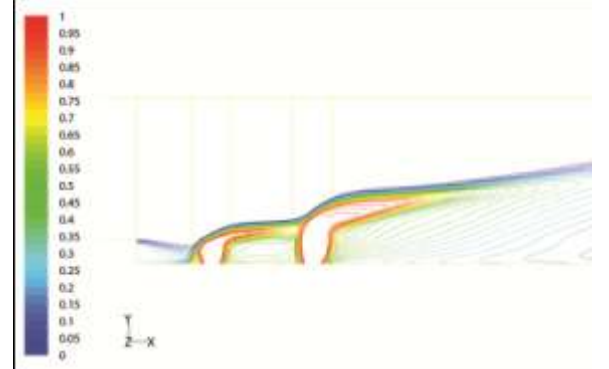


Fig15 :- Mole fraction of air(with

injection)

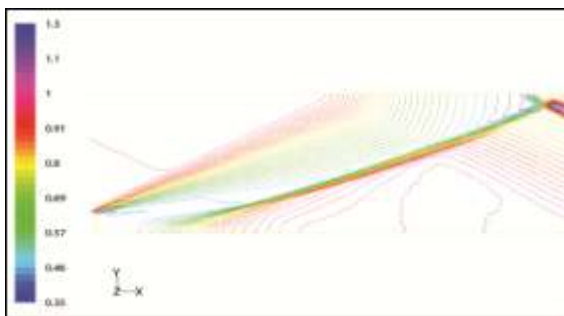


Fig16 :- P/P0 (without injection)
(without injection)

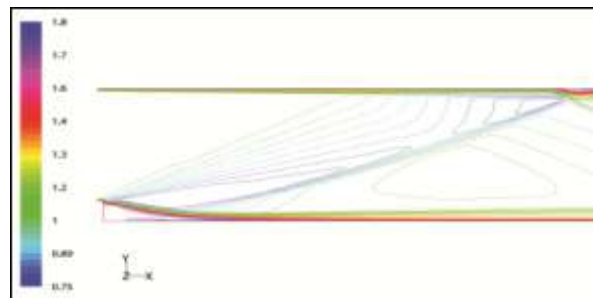


Fig17 :- T/T0

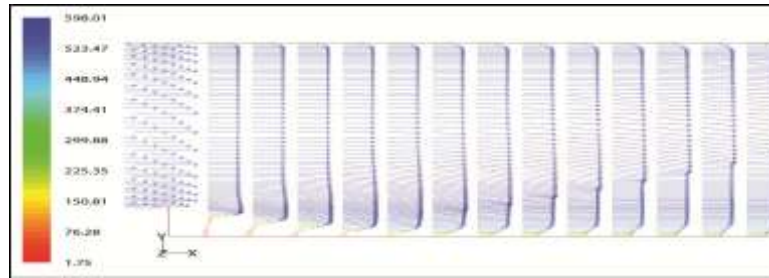


Fig18:-Velocity vector plot (without injection)
3)X-Y Plot

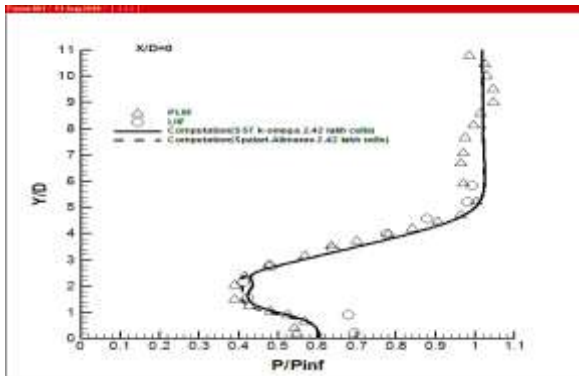


Fig19:-Comparison between Spalart-Allmaras pressure variation in transverse direction at X/D=0 (without injection)

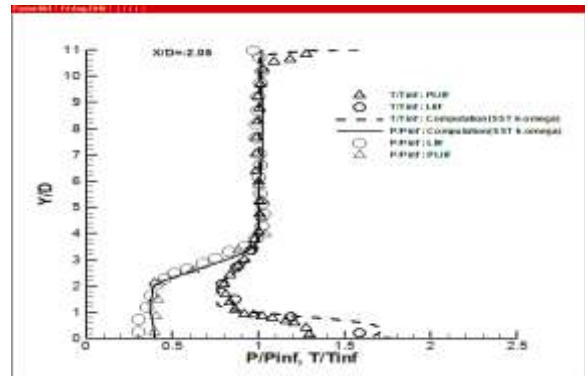


Fig20:-Temperature and SST K-omega schemes transverse direction at X/D=-2.05 (without injection)

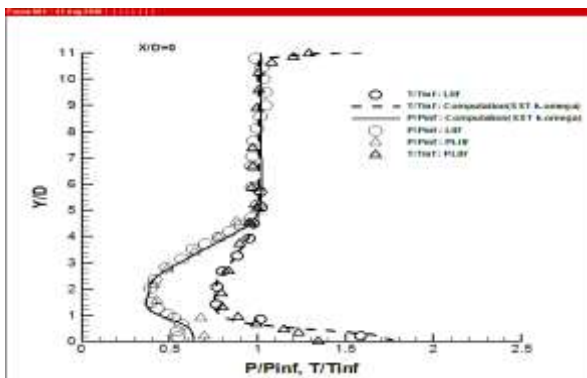


Fig21:- Temperature and pressure variation along transverse direction at X/D=0 (without injection)

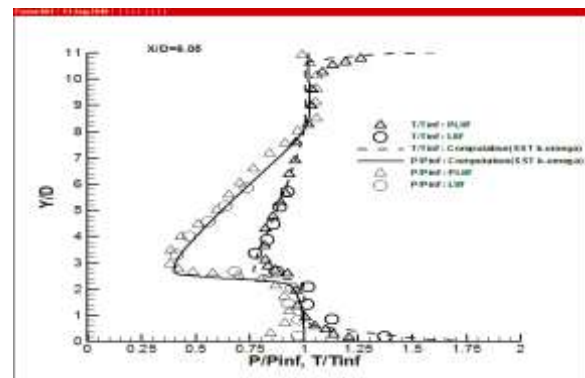


Fig22:- Temperature and pressure variation along transverse direction at X/D=6.05 (without injection)

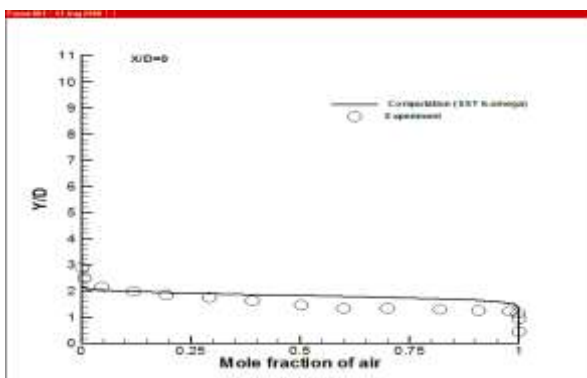


Fig23:- Variation of mole fraction of injectant in transverse direction at X/D=0 (With injection)

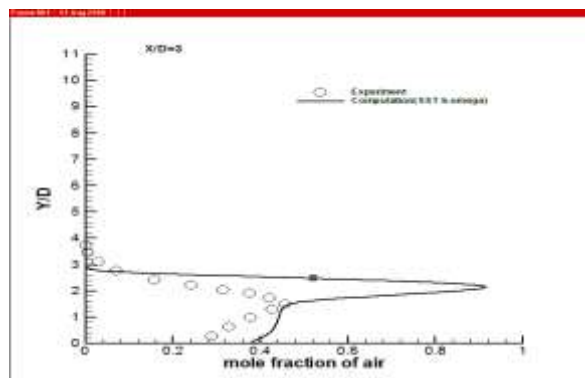


Fig24:- Variation of mole fraction of injectant in transverse direction at X/D=3 (With injection)

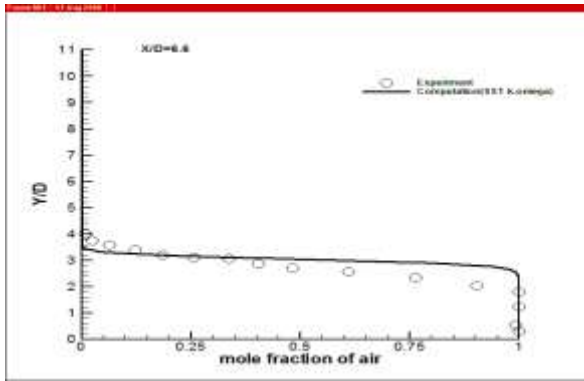


Fig25 :- Variation of mole fraction of injectant btw SST k-omega and Realizable k-epsilon(With injection) in transverse direction at X/D=6.6(With injection)

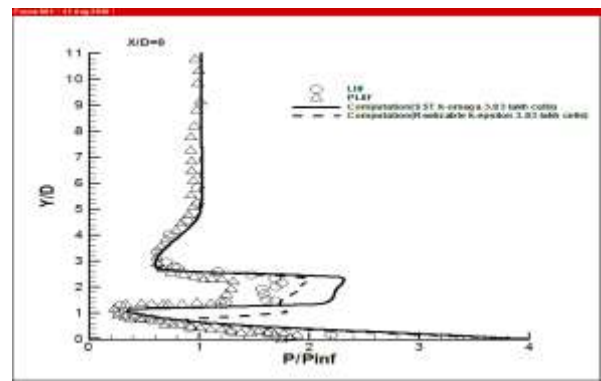


Fig 26 :- Comparison

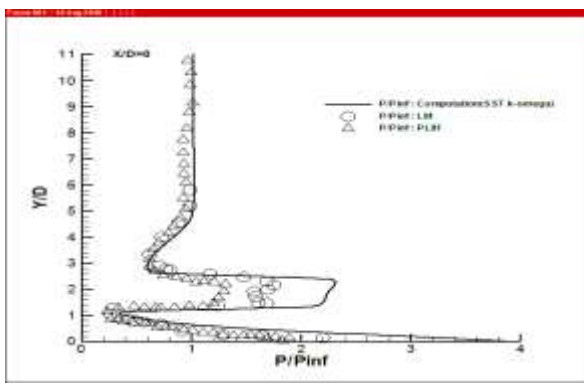


Fig27:- Pressure variation along transverse and pressure variation direction at X/D=0(with injection) transverse direction at X/D=3(with injection)

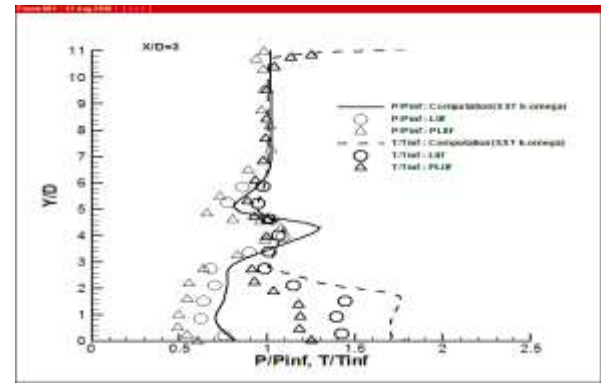


Fig28:- Temperature

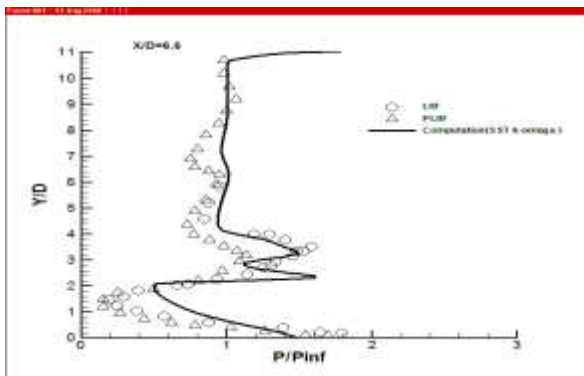


Fig29:-Pressure variation along transverse direction at X/D=6.6(with injection) variation along transverse direction at X/D=6.6(with injection)

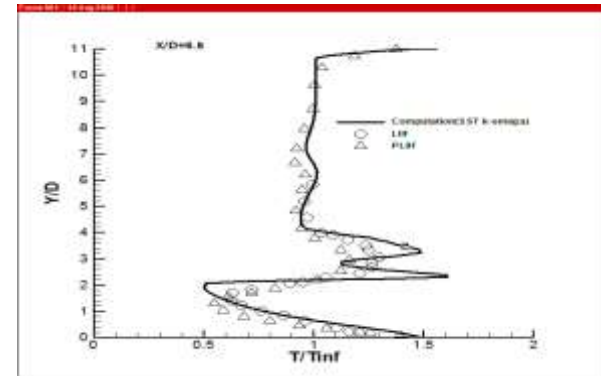


Fig30:-Temperature